Biochimie 152 (2018) 73–84

Contents lists available at ScienceDirect

Biochimie

journal homepage: www.elsevier.com/locate/biochi

Research paper

Dihydrodipicolinate synthase is absent in fungi

Sebastien Desbois [a], Ulrik P. John [a, b], Matthew A. Perugini [a, *]

[a] Department of Biochemistry and Genetics, La Trobe Institute for Molecular Science, La Trobe University, VIC, 3086, Australia
[b] Agriculture Victoria Research, Department of Economic Development, Jobs, Transport and Resources, AgriBio, La Trobe University, VIC, 3086, Australia

ARTICLE INFO

Article history:
Received 11 March 2018
Accepted 21 June 2018
Available online 27 June 2018

Keywords:
Class I aldolase
dapA gene
DHDPS
Lysine biosynthesis
Misannotation
Sequence motif

ABSTRACT

The class I aldolase dihydrodipicolinate synthase (DHDPS) catalyzes the first committed step of the diaminopimelate (DAP) lysine biosynthesis pathway in bacteria, archaea and plants. Despite the existence, in databases, of numerous fungal sequences annotated as DHDPS, its presence in fungi has been the subject of contradictory claims. We report the characterization of DHDPS candidates from fungi. Firstly, the putative DHDPS from *Coccidioides immitis* (PDB ID: 3QFE) was shown to have negligible enzyme activity. Sequence analysis of 3QFE showed that three out of the seven amino acid residues critical for DHDPS activity are absent; however, exact matches to catalytic residues from two other class I aldolases, 2-keto-3-deoxygluconate aldolase (KDGA), and 4-hydroxy-2-oxoglutarate aldolase (HOGA), were identified. The presence of both KDGA and HOGA activity in 3QFE was confirmed *in vitro* using enzyme assays, the first report of such dual activity. Subsequent analyses of all publically available fungal sequences revealed that no entry contains all seven residues important for DHDPS function. The candidate with the highest number of identities (6 of 7), KIW77228 from *Fonsecaea pedrosoi*, was shown to have trace DHDPS activity *in vitro*, partially restored by substitution of the seventh critical residue, and to be incapable of complementing DHDPS-deficient *E. coli* cells. Combined with the presence of all seven sequences for the alternative α-aminoadipate (AAA) lysine biosynthesis pathway in *C. immitis* and *F. pedrosoi*, we believe that DHDPS and the DAP pathway are absent in fungi, and further, that robust informed methods for annotating genes need to be implemented.

1. Introduction

The biosynthesis of lysine occurs in bacteria, archaea, fungi and plants using either the diaminopimelate (DAP) or α-aminoadipate (AAA) pathways [1–3]. However, lysine biosynthesis does not occur in animals, including mammals, who instead acquire this essential amino acid from dietary sources [4]. The first committed step of the DAP pathway (Fig. 1) is catalyzed by the class I aldolase, dihydrodipicolinate synthase (DHDPS) (EC 4.3.3.7). DHDPS condenses (*S*)-aspartate-4-semialdehyde (ASA) with pyruvate to form 4-hydroxy-2,3,4,5-tetrahydrodipicolinic acid (HTPA) [4–23]. This oligomeric enzyme is the product of the *dapA* gene, which has been shown through gene knock-out studies to be essential to bacteria [24,25] and plants [26]. However, there is no evidence to date demonstrating that DHDPS is essential to fungi. Indeed, previous reports imply that DHDPS is absent in fungi, since it is suggested that fungal species can only utilize the AAA pathway to synthesize lysine [2,27–29]; whereas other studies report that DHDPS is found in fungi as well as bacteria and plants [28,30–39].

The three-dimensional structure of DHDPS has been determined from 23 bacterial species, 2 plant species and 1 archaea to date (Table 1). These studies show that the DHDPS monomer forms a TIM- or $(\beta/\alpha)_8$-barrel with the active site located at the center of the barrel. Together with mutational studies, crystal structure analyses with bound substrate show that the DHDPS active site is comprised of seven conserved residues that are critical for function [20,21,37,46,62]. Firstly, a key lysine residue (Lys161, *Escherichia coli* numbering) is known to form a Schiff base with pyruvate, which is the first substrate to bind in the active site [8,37]. Three other residues, namely Thr44, Tyr107 and Tyr133 (*E. coli* numbering), align adjacent to one another and form a catalytic triad shuttling protons to and from the active site [8,20,62]. Interestingly, Thr44 and Tyr107 exist in dyad motifs with Thr45 and Tyr106,

* Corresponding author. Room 421, Level 4, La Trobe Institute for Molecular Science, La Trobe University, Kingsbury Drive, Bundoora, Melbourne, 3086, Australia.
E-mail address: M.Perugini@latrobe.edu.au (M.A. Perugini).

https://doi.org/10.1016/j.biochi.2018.06.017
0300-9084/

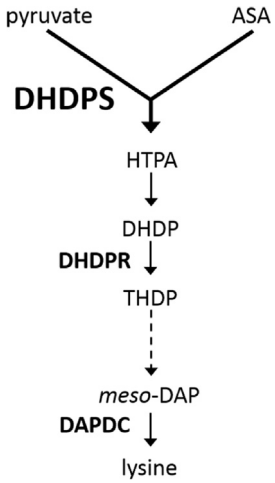

Fig. 1. Diaminopimelate (DAP) biosynthesis pathway. The DAP pathway commences with the condensation of pyruvate with (*S*)-aspartate-4-semialdehyde (ASA) to form 4-hydroxy-2,3,4,5-tetrahydrodipicolinic acid (HTPA) catalyzed by dihydrodipicolinate synthase (DHDPS). HTPA is then non-enzymatically dehydrated to yield dihydrodipicolinate (DHDP), which is then reduced by dihydrodipicolinate reductase (DHDPR) to yield (*S*)-2,3,4,5-tetrahydrodipicolinate (THDP). At this point, the DAP pathway branches out into 4 different subpathways depending on species using multiple enzymes. All 4 subpathways reunite with the formation of *meso*-diaminopimelate (*meso*-DAP), which is decarboxylated by the diaminopimelate decarboxylase (DAPDC) to form the end product (*S*)-lysine.

respectively, which are both highly conserved in all bacterial and plant DHDPS sequences characterized to date [13,16,17,63,64]. There is also a conserved arginine, Arg138 (*E. coli* numbering), that acts as a gate keeper residue facilitating the entry of both pyruvate and ASA into the active site [46,64].

In bacteria, the DHDPS monomer self-associates to form either functional dimers [14,55,58] or tetramers [9,15,18,62,65] that adopt the structures shown in Fig. 2A and Fig. 2B, respectively. By contrast, plant DHDPS enzymes also form tetramers, but in a back-to-back dimer-of-dimer arrangement (Fig. 2C) compared to the head-to-head architecture observed for bacterial tetramers (Fig. 2B). Recently, a crystal structure of a putative fungal DHDPS (PDB ID: 3QFE) has been deposited in the Protein Data Bank (PDB) (Fig. 2D) from the human pathogen *Coccidioides immitis* [66–68]. However, no functional data has been reported to validate 3QFE as a DHDPS enzyme. Although the structure of 3QFE shows a tetramer (Fig. 2D), the quaternary form of this enzyme differs in architecture from the canonical bacterial (Fig. 2B) and plant (Fig. 2C) tetrameric forms. Nevertheless, numerous fungal genomes have been annotated to include DHDPS sequences (www.ncbi.nlm.nih.gov) suggesting that the DAP pathway occurs in some fungi.

Most bacterial species contain one *dapA* gene [24,51,63]; whilst plants commonly contain two *dapA* genes [16,22,26,69–72]. Surprisingly, it was thought based on genome annotation that the Gram negative bacterium, *Agrobacterium tumefaciens*, contained 10 *dapA* genes [63]. However, structure and function studies demonstrated that only one of these genes (*dapA7*) encoded a functional DHDPS (PDB ID: 4I7U) [63]. Of the other 9 putative DHDPS-encoding genes, it has recently been demonstrated that the *dapA5* gene encodes a 2-keto-3-deoxygluconate aldolase (KDGA) (EC 4.1.2.20) [73]. The remaining 8 genes are likely to encode other class I aldolases, such as 4-hydroxy-2-oxoglutarate aldolase (HOGA) (EC 4.1.3.16), *N*-acetylneuraminate lyase (NAL) (EC 4.1.3.3) and *trans*-20-carboxybenzalpyruvate hydratase aldolase (EC 4.1.2.45) [63].

In this study, we set out to validate that 3QFE possesses DHDPS enzymatic activity, and secondly, ascertain whether other putative fungal *dapA* genes encode an active DHDPS. We report here that 3QFE lacks DHDPS catalytic function, and instead possesses dual HOGA and KDGA enzymatic activity. We subsequently show, using bioinformatics analyses, that no extant fungal genome contains *dapA* gene(s), providing strong evidence that fungi do not utilize the DAP pathway to synthesize lysine. We also describe a 7 residue signature motif that can be used to identify *bona fide* DHDPS sequences. This will aid in correctly annotating *dapA* gene or DHDPS protein entries in future sequencing projects.

Table 1
List of all PDB IDs of structures from confirmed DHDPS enzymes to date.

Kingdom	Species	PDB IDs	Citation (if available)
Eubacteria	*Acinetobacter baumannii*	3PUD, 3PUE, 3PUL, 3RK8, 3TAK, 3TCE, 3TDF, 3U8G, 3UQN, 4DVX	
	Agrobacterium tumefaciens	4I7U, 4I7V, 4I7W	
	Anabaena variabilis	5KTL	[40]
	Aquifex aeolicus	2EHH	
	Bacillus anthracis	1XKY, 1XL9, 3HIJ	[13,18]
	Bacillus clausii	3E96	
	Bartonella henselae	3SI9	[41]
	Campylobacter jejuni	3LER, 3M5V, 4LY8, 4M19, 4MLJ, 4MLR, 4R53, 5F1U, 5F1V	[42,43]
	Clostridium botulinum	3IRD	
	Corynebacterium glutamicum	3CPR	[44]
	Escherichia coli	1DHP, 1S5T, 1S5V, 1S5W, 1YXC, 1YXD, 2A6L, 2A6N, 2ATS, 2OJP, 2PUR, 3COJ, 3DEN, 3DUO, 3I7Q, 3I7R, 3I7S, 4EOU, 5T25, 5T26	[9,12,15,45–51]
	Hahella chejuensis	2RFG	
	Mycobacterium tuberculosis	1XXX, 3L21, 5J5D	[52,53]
	Neissiria meningitidis	3FLU	[54]
	Oceanobacillus iheyensis	3D0C	
	Pseudomonas aeruginosa	3NA8, 3NOE, 3PS7, 3PUO, 3QZE, 3S8H	[55,56]
	Rhizobium meliloti	2VC6	
	Rhodopseudomonas palustris	3DZ1, 3EB2	
	Salmonella typhimurium	3G0S	
	Shewanella benthica	4ICN, 4PFM	
	Staphylococcus aureus	2D5K, 3DI0, 3DI1, 3DAQ	[57,58]
	Thermotoga maritima	1O5K, 3PB0, 3PB2	[59]
	Thermus thermophilus	2PCQ	
Planta	*Arabidopsis thaliana*	4DPP, 4DPQ	[60]
	Vitis vinifera	3TUU	[37]
Archaea	*Methanocaldococcus jannaschii*	2YXG	[61]

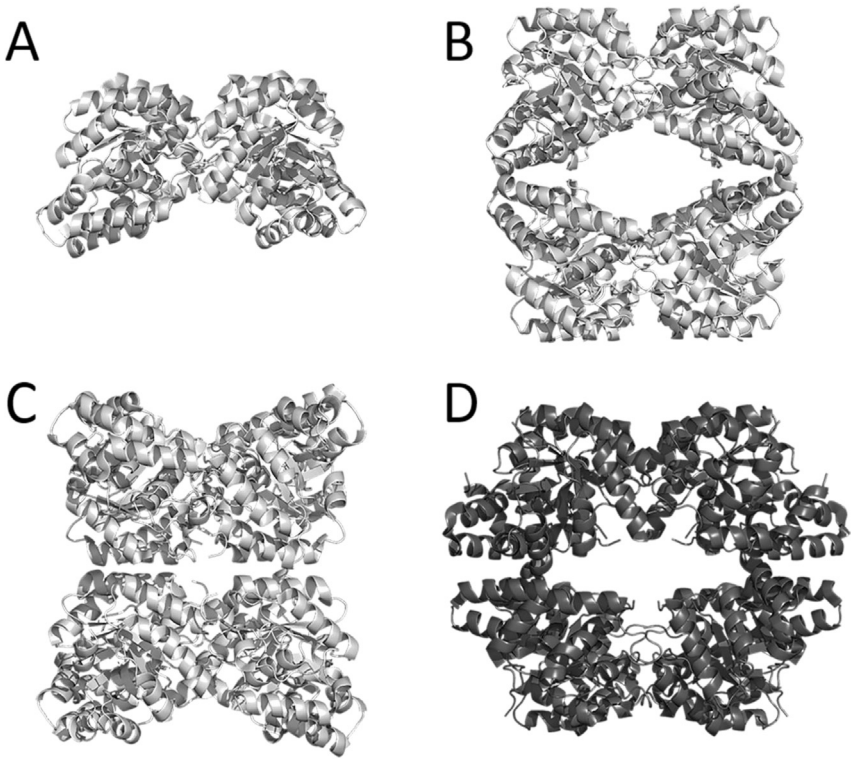

Fig. 2. Crystal structures of bacterial, plant and putative fungal DHDPS enzymes. (A) *Staphylococcus aureus* DHDPS (PDB ID: 3DAQ) is present as a homodimer in solution whilst (B) the canonical structure of bacterial species like that of *E. coli* (PDB ID: 1YXC) forms a head-to-head tetramer. (C) Plant DHDPS enzymes also form tetramers but with a canonical back-to-back architecture as found in *Vitis vinifera* (PDB ID: 3TUU). (D) The crystal structure of the putative DHDPS from the fungus *Coccidioides immitis* (PDB ID: 3QFE) differs from the canonical bacterial and plant architectures.

2. Materials and methods

2.1. Materials

Unless otherwise stated, all chemicals were purchased from Sigma-Aldrich. Plasmids (pET28) containing the genes (codon optimized for *E. coli*) encoding 3QFE and KIW77228 were synthesized by Bioneer Pacific. Plasmid (pBLUE-Script) containing the gene encoding *E. coli* DHDPS was kindly provided by Prof Juliet Gerard (University of Auckland, NZ); and the plasmid (pET11) containing the gene for *S. aureus* NAL was a kind gift from A/Prof Renwick Dobson (University of Canterbury, NZ). To be consistent, all genes used for recombinant protein expression in this study were sub-cloned into pET28 vectors (where appropriate). AT997r^{-} strain was kindly provided by A/Prof Ashley Franks (La Trobe University, Australia).

2.2. In vitro mutagenesis

The A138R (i.e. GCA → CGT) mutation of the *Fonsecaea pedrosoi kiw77228* gene (encoding KIW77228 protein) was introduced by employing the QuickChange® protocol using Phusion DNA polymerase and *Dpn*I enzymes (New England Biolabs) according to the manufacturer's instructions. Primers (Forward: GTATTATAACATTCCGAGCCGTAGCGGTCTGAGCCTGACC; Reverse: GGTCAGGCTCAGACCGCTACGGCTCGGAATGTTATAATAC) were designed using primerX (www.bioinformatics.org/primerx/) and the codon for the mutation was selected for optimized expression in *E. coli* cells [74]. Plasmid inserts were confirmed using Sanger dideoxy sequencing [75] performed commercially by the Australian Genome Research Facility (AGRF).

2.3. Protein expression and purification

Recombinant proteins were over-expressed in *E. coli* BL21 (DE3) transformed with the desired plasmid. Protein expression was induced following treatment with 0.5 mM isopropyl β-D-1-thiogalactopyranoside (IPTG) in Luria Broth (LB) at 37 °C for 4 h. The cells were pelleted by centrifugation (4000 × g), supernatant discarded, and cell pellet re-suspended in immobilized metal affinity liquid chromatography (IMAC) binding buffer (20 mM Tris, 500 mM NaCl, 10 mM imidazole, pH 8.0). The cell suspension was sonicated (Qsonica Q700 & 12.7 mm probe) and the resulting cell lysate loaded onto a 5 ml Bio-Scale™ Mini Profinity™ IMAC Cartridge column (BIO-RAD). The unbound protein was washed from the column using 6 column volumes of IMAC binding buffer, followed by a second 6 column volume wash with 20 mM Tris, 500 mM NaCl and 20 mM imidazole pH 8.0 before the bound protein was eluted with 20 mM Tris, 500 mM NaCl, 500 mM imidazole, pH 8.0. The fractions containing pure (>98% purity) recombinant protein as assessed by SDS-PAGE [76] were pooled and buffer exchanged into 20 mM Tris, 150 mM NaCl (pH 8.0) using a 50 ml Bio-Scale™ Mini Bio-Gel® P-6 Desalting Cartridge.

2.4. Mass spectrometry

Prior to mass spectrometry (MS) analysis, formic acid was added to solutions of purified recombinant protein to a final concentration of 1.3% (v/v). MS was performed by direct injection on a hybrid quadrupole time-of-flight (Micro-TOF-Q) mass spectrometer with an electrospray ionization (ESI) source (Bruker-Daltonics). The spectra were acquired in positive ion mode using an ionization tip voltage of 4200 V and an interface temperature at 280 °C. The

nebulizer was set to 0.7 bar with a dry gas flow rate of 8 L/min. Both the transfer funnel radio frequency (RF) and multipole RF were fixed at 400 Vpp. The quadrupole ion energy, collision cell energy and collision RF were 5 eV, 10 eV and 1800 Vpp, respectively. Finally, the ion cooler transfer time was 90 μs with a pre-pulse storage of 5 μs. Raw data were processed using Bruker Compass DataAnalysis 4.0, and deconvolution performed using the Maximum Entropy algorithm with a mass range of 1,000–100,000 Da and normal resolution.

2.5. Circular dichroism spectroscopy

Circular dichroism (CD) spectra of 3QFE, KIW77228 and KIW77228-A138R solubilized in 20 mM Tris, 150 mM NaCl, pH 8.0 at a concentration of 0.15 mg/ml were recorded on an Aviv Model 420 CD spectrometer using similar methods reported previously [18,37,40,63,73]. Briefly, wavelength scans were collected at 20 °C between 195 and 260 nm using a step-size of 0.5 nm and a signal averaging time of 4.0 s. Raw data were converted to mean residue ellipticity (MRE) and subsequently fitted by nonlinear regression using CDPRO software employing the SP22X and SP29 databases and CONTINLL algorithm [77,78].

2.6. Enzymatic coupled assays

2.6.1. DHDPS-DHDPR coupled assay

Assays were performed in 250 mM HEPES, pH 8.0 containing excess amounts of NADPH (0.2 mM), dihydrodipicolinate reductase (DHDPR) (31.5 μM), pyruvate (2.5 mM) and ASA (1 mM) as previously described [5,12,14,18,21,63,79,80]. Briefly, the initial rate of the reaction was determined by monitoring the decrease in absorbance at 340 nm as a function of time. Each reaction was allowed to equilibrate at 37 °C for 12 min before the addition of ASA to initiate the reaction. All assays were performed in triplicate (n = 3).

2.6.2. NAL-LDH coupled assay

Assays were performed in 50 mM sodium phosphate, pH 8.0 containing excess amounts of NADH (0.4 mM), lactate dehydrogenase (LDH) (6.7 μM) and substrate *N*-acetylneuraminic acid (Neu5Ac) (12 mM) as described previously [81]. The temperature, pH and buffer were selected based on optimum activity of LDH from porcine heart [73]. Briefly, buffer, enzymes and cofactor were equilibrated together at 37 °C for 12 min before the addition of Neu5Ac to initiate the reaction. The initial rate was then determined by measuring the reduction in absorbance at 340 nm at concentrations of NAL ranging from 0 to 12.5 μg/ml. All assays were performed in triplicate (n = 3).

2.6.3. KDGA-LDH coupled assay

Assays were performed in 50 mM sodium phosphate, pH 8.0 containing excess amounts of NADH (0.4 mM), LDH (6.7 μM) and substrate 2-keto-3-deoxygluconate (KDG) (2 mM) as described previously [73]. The temperature, pH and buffer were selected based on optimum activity of LDH from porcine heart [73]. Briefly, buffer, enzymes and cofactor were equilibrated together at 37 °C for 12 min before the addition of KDG to initiate the reaction. The initial rate was then determined by measuring the reduction in absorbance at 340 nm at concentrations of KDGA ranging from 0 to 375 μg/ml. All assays were performed in triplicate (n = 3).

2.6.4. HOGA-LDH coupled assay

Assays were performed in 50 mM sodium phosphate, pH 8.0 containing excess amounts of NADH (0.4 mM), LDH (6.7 μM) and substrate 4-hydroxy-2-oxoglutarate (HOG) (0.8 mM) as described previously [82,83]. The temperature, pH and buffer were selected based on optimum activity of LDH from porcine heart [73]. Briefly, buffer, enzymes and cofactor were equilibrated together at 37 °C for 12 min before the addition of HOG to initiate the reaction. The initial rate was then determined by measuring the reduction in absorbance at 340 nm at concentrations of HOGA ranging from 0 to 25 μg/ml. All assays were performed in triplicate (n = 3).

2.7. Complementation assay

The complementation assay was performed by transforming the *E. coli dapA* knock-out mutant strain AT997r$^-$ [15,84–86] with pET28a vectors carrying either *F. pedrosoi kiw77228*, *C. immitis 3qfe* or *E. coli dapA* as well as an empty pET28a vector as a control. AT997r$^-$ cells were grown at 37 °C (shaking at 160 rpm) in LB media supplemented with 500 μM DAP and 35 μg/ml kanamycin until the culture reached an OD_{600nm} of 0.6 at which point the cells were harvested by centrifugation (4000 × g). The cell pellet was re-suspended in the same volume of LB containing 35 μg/ml kanamycin and either 500 μM DAP (positive control) or 0.5 mM IPTG to induce recombinant protein expression to support growth (where applicable). After incubation at 37 °C for 15 min, 100 μl of culture was plated onto LB agar containing 35 μg/ml kanamycin and either 500 μM DAP or 0.5 mM IPTG. Plates were then incubated at 37 °C overnight.

2.8. Phylogenetic analysis

Selected sequences from multiple kingdoms with validated DHDPS, HOGA, KDGA and NAL enzymatic function were aligned using ClustalW [87], and both neighbor joining (NJ) [88] and maximum likelihood (ML) [89,90] phylogenetic trees were constructed using Mega version 6 [91]. The NJ tree was obtained through the Poisson model [92] with 10,000 bootstrap replications, and the ML tree through the Jones-Taylor-Thornton model [93] using the Nearest-Neighbor-Interchange Heuristic method [94,95] also employing 10,000 bootstrap replications. The phylogenetic trees were compiled using FigTree version 1.4.3 (http://tree.bio.ed.ac.uk/software/figtree/).

3. Results and discussion

3.1. Expression, purification and structural characterization of recombinant 3QFE

Recombinant His-tagged 3QFE was overexpressed in *E. coli* BL21 (DE3) cells and purified by IMAC to yield 23 mg of >98% pure protein per liter of culture. The recombinant product was shown by ESI Q-TOF mass spectrometry to have a molecular mass of 36,525.5 Da, which is in excellent agreement with the theoretical molecular mass of the monomeric sequence (M_r = 36,525.1). CD spectroscopy was subsequently employed to show that the recombinant protein was folded to form a mixed α/β structure, which is consistent with the crystal structure of the protein (Fig. 2D). We therefore set out to determine if the folded 3QFE recombinant product possesses DHDPS catalytic function.

3.2. 3QFE lacks DHDPS function

DHDPS enzymatic activity was assessed using the DHDPS-DHDPR coupled assay [5,12,14,18,21,63,79,80]. Fig. 3 shows a plot of raw activity ($\Delta A_{340\,nm}$/min) as a function of protein concentration. The control, *E. coli* DHDPS, shows a typical rate versus enzyme concentration relationship that is linear at low protein concentration and begins to plateau at higher concentration when the

substrates become limiting (Fig. 3, triangles). However, the rate versus protein concentration profile for 3QFE shows negligible activity across the same protein concentration range employed for the control (Fig. 3, squares). This indicates that 3QFE lacks DHDPS catalytic function. We therefore set out to carefully examine the sequence of 3QFE to identify potential signature motifs that would reveal the function of this fungal protein.

3.3. Multiple sequence analyses comparing 3QFE to known class I aldolases

Initially, we aligned the protein sequences of 3QFE with known DHDPS enzymes. A multiple, partial sequence alignment including the key conserved catalytic residues (gray shadowing) is shown in Fig. 4A. Not surprisingly, 3QFE lacks 3 of the 7 conserved residues known to be important for conferring DHDPS function [9,12,45,48]. Specifically, 3QFE contains an asparagine instead of a threonine at position 45 (*E. coli* numbering), an alanine replaces a tyrosine at position 106, and valine is located at position 138 instead of arginine. We then aligned the protein sequences of 3QFE with other class I aldolase enzymes related to DHDPS, namely NAL, KDGA and HOGA. The suggested catalytic residues for each enzyme (gray shadowing) are shown in the resulting multiple sequence alignment (Fig. 4B). Interestingly, 3QFE lacks 3 out of 7 residues known to be important for NAL activity [81,96–100], namely Ser, Thr, and Glu at positions 44, 45 and 189 are instead Thr, Asn and Asp, respectively. However, 3QFE possesses all the residues necessary for both KDGA and HOGA activity (Fig. 4B). Only 3 conserved catalytic residues are common to KDGA and HOGA, namely Tyr107, Tyr133 and Lys161; while Thr44 and Thr163 are specific to KDGA, and Asn45, Arg64 and Pro155 are specific to HOGA (Fig. 4B).

3.4. Class I aldolase assays show 3QFE possesses dual HOGA and KDGA activity

Given the sequence similarity with HOGA and KDGA, we next set out to determine if 3QFE functions as one or both of these class I aldolases. Using the HOGA-LDH coupled assay, we show that 3QFE possesses significant HOGA activity (Fig. 5A) as predicted. Indeed, the level of HOGA enzymatic activity is comparable to rates previously described for mammalian orthologs [82,101]. Interestingly, 3QFE also displays significant KDGA activity (Fig. 5B) with rates

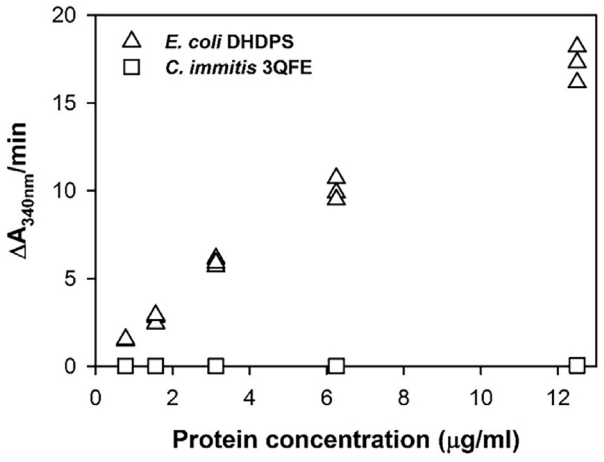

Fig. 3. DHDPS activity of 3QFE as a function of protein concentration. The DHDPS-DHDPR coupled assay was used to determine DHDPS activity of 3QFE (squares) relative to the *E. coli* control (triangles). The $\Delta Abs_{340\,nm}$/min is plotted as a function of protein concentration, n = 3.

consistent with earlier studies [73]. This is unusual given that class I aldolases are renowned for being highly specific for their substrate, including strict stereoselectivity [102–104]. However, there are rare reports in the literature of non-specific class I aldolases. For example, a KDGA from *Sulfolobus solfataricus* has been shown to possess dual activity for unphosphorylated and phosphorylated substrates [105,106]. Similarly, a class I aldolase has previously been demonstrated to possess dual fructose-bisphosphate aldolase and sedoheptulose-bisphosphate aldolase activity in both archaea [107] and higher plants [108]. Nevertheless, we believe that this is the first description of a class I aldolase that possesses dual HOGA and KDGA functionality. We also determined if 3QFE possesses NAL enzymatic activity, but found that 3QFE lacks NAL functionality compared to the *S. aureus* NAL control (Fig. 5C).

3.5. Is DHDPS found in other fungal species?

Having shown that 3QFE does not possess DHDPS activity, we next set out to determine whether fungal species in general contain a *bona fide* DHDPS enzyme. A Pattern Hit Initiated BLAST [109] against the fungal database using the 7-residue DHDPS motif (Fig. 4A) failed to produce any hits, indicating that no current publicly available fungal sequence possesses all 7 residues critical for DHDPS function. To confirm this, we also performed a BLASTP [110] search against the fungal database using the *E. coli* DHDPS sequence. The results (Fig. S1) reveal that all but two sequences contain 5 or less of the 7 conserved DHDPS catalytic residues. Of the two sequences that possess 6 of the 7 residues, namely the 6th and 7th ranked entries, only KIW77228 from *Fonsecaea pedrosoi* (Fig. S1, boxed), a human pathogen [111], is annotated as a DHDPS (i.e. *dapA* product). We set out to explore whether this was true by expressing and purifying KIW77228 to assess its potential DHDPS functionality.

3.6. Expression, purification and characterization of recombinant KIW77228

KIW77228 was overexpressed in *E. coli* BL21 (DE3) cells as an amino-terminal His-tagged construct and purified by IMAC to yield 14 mg of >98% pure protein per liter of culture. The recombinant product was shown by ESI Q-TOF mass spectrometry to have a molecular mass of 35,505.1 Da, which is in excellent agreement with the theoretical molecular mass of the monomeric sequence ($M_r = 35{,}504.5$). CD spectroscopy was then employed to show that the recombinant protein formed a mixed α/β structure, consistent with other TIM-barrel enzymes [14,18,25,40,73]. Having demonstrated the recombinant product was comprised of the correct sequence and was folded, we next examined whether KIW77228 possessed DHDPS catalytic function. DHDPS activity was measured using the coupled assay [5,12,21,63,79,80] at increasing protein concentrations. The resulting data plotted as raw activity ($\Delta A_{340\,nm}$/min) versus protein concentration shows negligible DHDPS activity for KIW77228 (Fig. 6A, triangles) relative to the *E. coli* DHDPS control (Fig. 3). To confirm this result, we performed complementation assays using the DHDPS-deficient strain of *E. coli*, AT997r$^-$ [15,84–86]. This strain was transformed with plasmids expressing KIW77228 or 3QFE, as well as *E. coli* DHDPS and an empty plasmid as controls. As expected, all transformed cells grew on DAP-supplemented plates (Fig. 6B), while only the cells transformed with the plasmid encoding *E. coli* DHDPS was able to grow (Fig. 6C). This indicates that 3QFE cannot complement DHDPS, which is consistent with our enzyme kinetics studies (Fig. 3). Likewise, KIW77228 cannot complement the AT997r$^-$ strain. This demonstrates that although KIW77228 is only lacking one of the seven residues of the DHDPS catalytic motif, the presence of Arg at

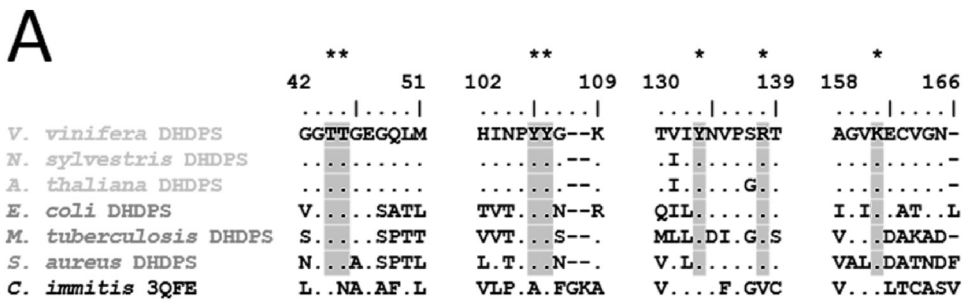

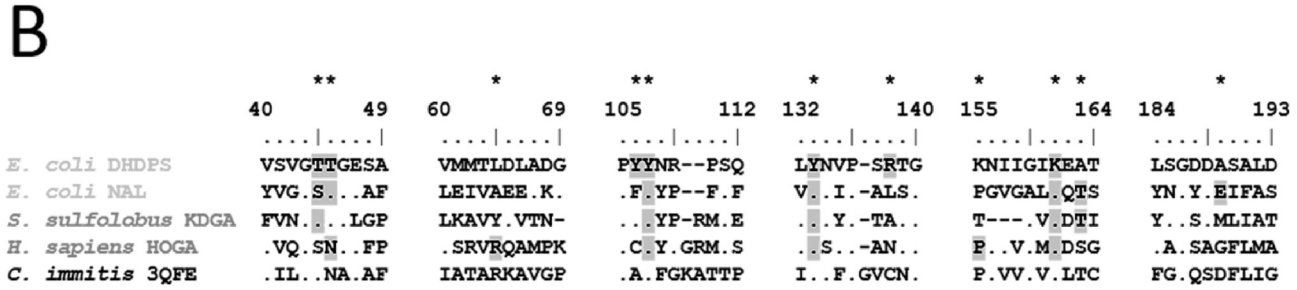

Fig. 4. Multiple sequence alignments of 3QFE. (A) The 3QFE sequence was aligned with the DHDPS sequences from 3 plant species, *Vitis vinifera*, *Nicotiana sylvestris*, *Arabidopsis thaliana* and 3 bacterial species *E. coli*, *Mycobacterium tuberculosis* and *S. aureus*. The dots represent conserved residues and the dashes represent gaps relative to the *V. vinifera* sequence. All numbering is based on the *E. coli* DHDPS sequence. The gray highlighted residues represent the key 7 residue signature motif critical for DHDPS catalytic activity. (B) The 3QFE sequence aligned with other class I aldolases (DHDPS, *N*-acetylneuraminate lyase (NAL), 2-keto-3-deoxygluconate aldolase (KDGA) and 4-hydroxy-2-oxoglutarate aldolase (HOGA)) relevant to this study from either Eubacteria (*E. coli*), Archaea (*Sulfolobus solfataricus*) or Animalia (*Homo sapiens*). The sequence dots indicate conserved residues and dashes represent gaps relative to the *E. coli* DHDPS sequence. The residues highlighted with gray shadowing are the suggested catalytic residues for each enzyme. All numbering is based on the *E. coli* DHDPS sequence.

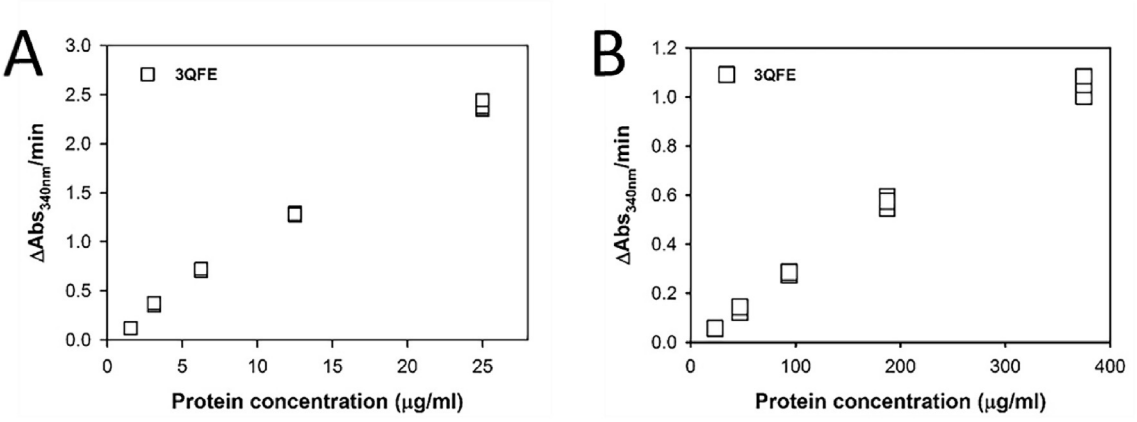

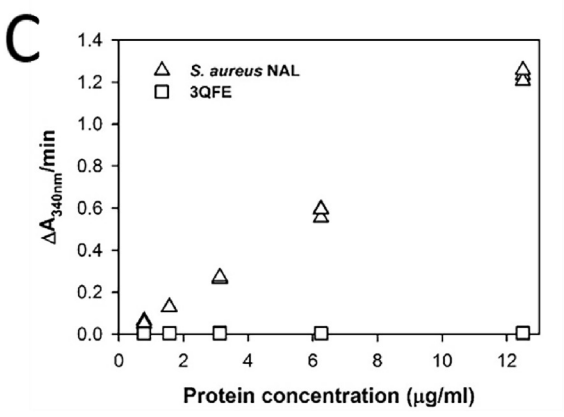

Fig. 5. 3QFE activity for different class I aldolase functions. The $\Delta Abs_{340\,nm}$/min is plotted as a function of protein concentration, n = 3. (A) The HOGA activity of 3QFE (squares) was tested using the HOGA-lactate dehydrogenase (LDH) coupled assay. (B) Likewise, the KDGA activity of 3QFE (squares) was tested using the KDGA-LDH coupled assay. (C) Finally, the NAL activity of 3QFE (squares) was tested using the NAL-LDH coupled assay with *S. aureus* NAL (triangles) as a control.

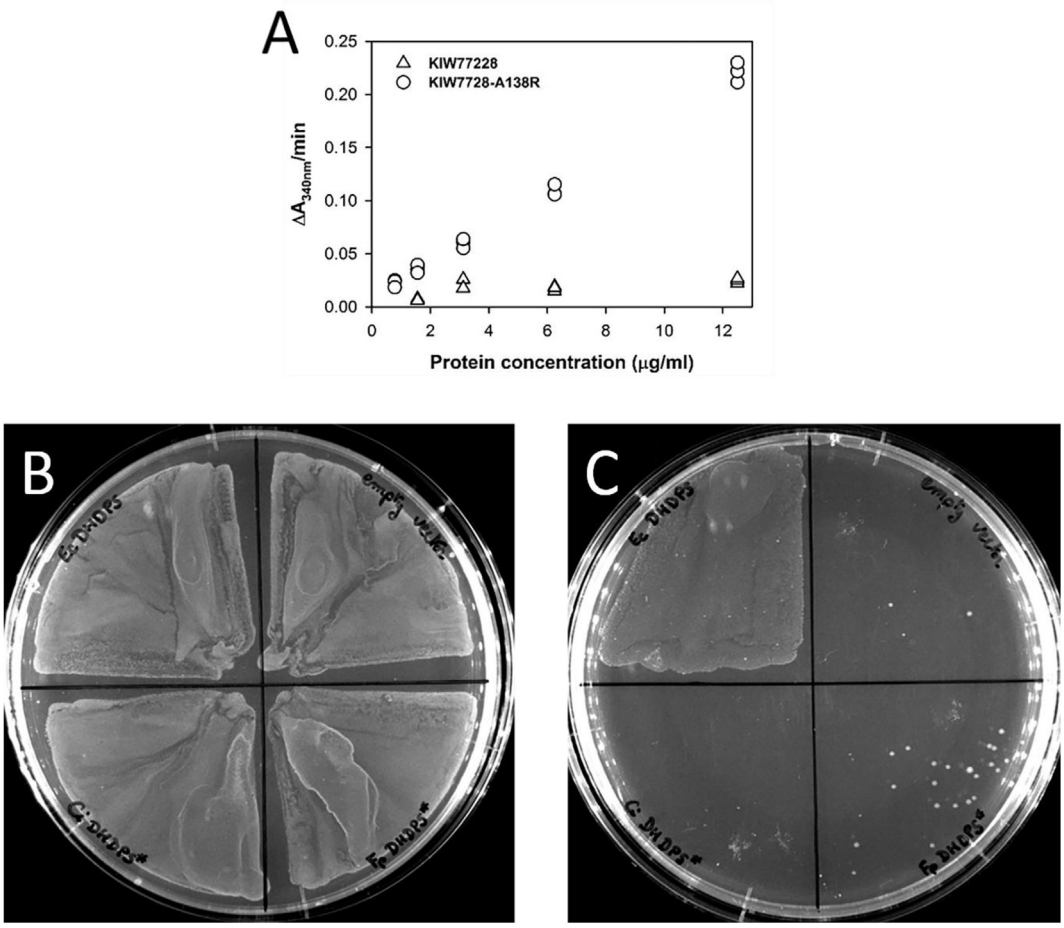

Fig. 6. DHDPS activity of KIW77228. (A) The DHDPS-DHDPR coupled assay was used to determine the DHDPS catalytic activity of KIW77228 (triangles) and KIW77228-A138R mutant (circles). The $\Delta Abs_{340\,nm}$/min is plotted as a function of protein concentration, n = 3. (B–C) Agar plate results of complementation assay of DHDPS-deficient (AT997r$^-$) *E. coli* cells with KIW77228. AT997r$^-$ *E. coli* cells were transformed with a vector expressing *E. coli* DHDPS (top left quadrant), 3QFE (bottom left quadrant), KIW77228 (bottom right quadrant) and an empty vector (top right quadrant). The cells were grown on (B) DAP-enriched Luria-Broth (LB) media or (C) grown on LB media with IPTG overnight.

position 138 (*E. coli* numbering) is essential for DHDPS function. To confirm this, we employed site-directed mutagenesis to engineer a KIW77228 point mutant that contained Arg at position 138 instead of Ala (KIW77228-A138R). 12 mg of >98% pure recombinant KIW77228-A138R was expressed per liter of culture. Mass spectrometry and CD spectroscopy were once again utilized to demonstrate the mutant protein was comprised of the correct primary structure and was folded with similar secondary structure to the wild-type KIW77228 recombinant product. In the DHDPS-DHDPR coupled assay, KIW77228-A138R (Fig. 6A) was observed to possess significant DHDPS catalytic function, with 10-fold greater activity than wild-type KIW77228 (Fig. 6A); although the mutant remains 70-fold less active than the *E. coli* DHDPS control (Fig. 3).

3.7. Phylogenetic analysis of 3QFE and KIW77228

To provide further insight into the evolutionary divergence of class I aldolases of relevance to this study, we performed a rooted phylogenetic analysis of DHDPS, HOGA, KDGA and NAL enzymes (Fig. 7). Sequences were selected from different kingdoms, including Animalia, Archaea, Chromista, Eubacteria and Planta. All together there were 72 sequences used in this analysis, including 3QFE and KIW77228. Both the NJ and ML trees resulted in an identical topology, thus only the NJ tree is represented here (Fig. 7). The phylogenetic trees showed that all DHDPS sequences cluster together, but are differentiated into sub-clusters according to their kingdom of origin (Fig. 7, different colored clades). The DHDPS sequences are the sister clade to the HOGA enzymes, which is consistent with previous studies [82]. The NAL sequences, only available for Animalia and Eubacteria, also cluster together, but are differentiated in a kingdom-dependent manner. Finally, the KDGA sequences, although not extensively available, appear to have two independent origins. Indeed, the Eubacteria KDGA sequences are phylogenetically closer to the HOGA and DHDPS clades compared to the Archaea KDGA sequences, which are more closely aligned with the NAL branch. Neither 3QFE nor KIW77228 cluster with the DHDPS enzymes, which is consistent with the aforementioned results of this study. More specifically, 3QFE clusters within the HOGA clade, while KIW77228 does not fit into any of the clades, but instead sits in a monotypic cluster diverging early from the super-cluster that includes DHDPS, HOGA and Eubacterial KDGA.

3.8. DAP pathway is not found in fungi

Both kinetic (Figs. 3 and 6) and phylogenetic (Fig. 7) data presented here indicates that DHDPS is not present in the Fungi kingdom. Indeed, even the most similar fungal sequence, containing 6 of the 7 key residues known to be important for DHDPS function, was shown to lack DHDPS activity (Fig. 6). Additionally,

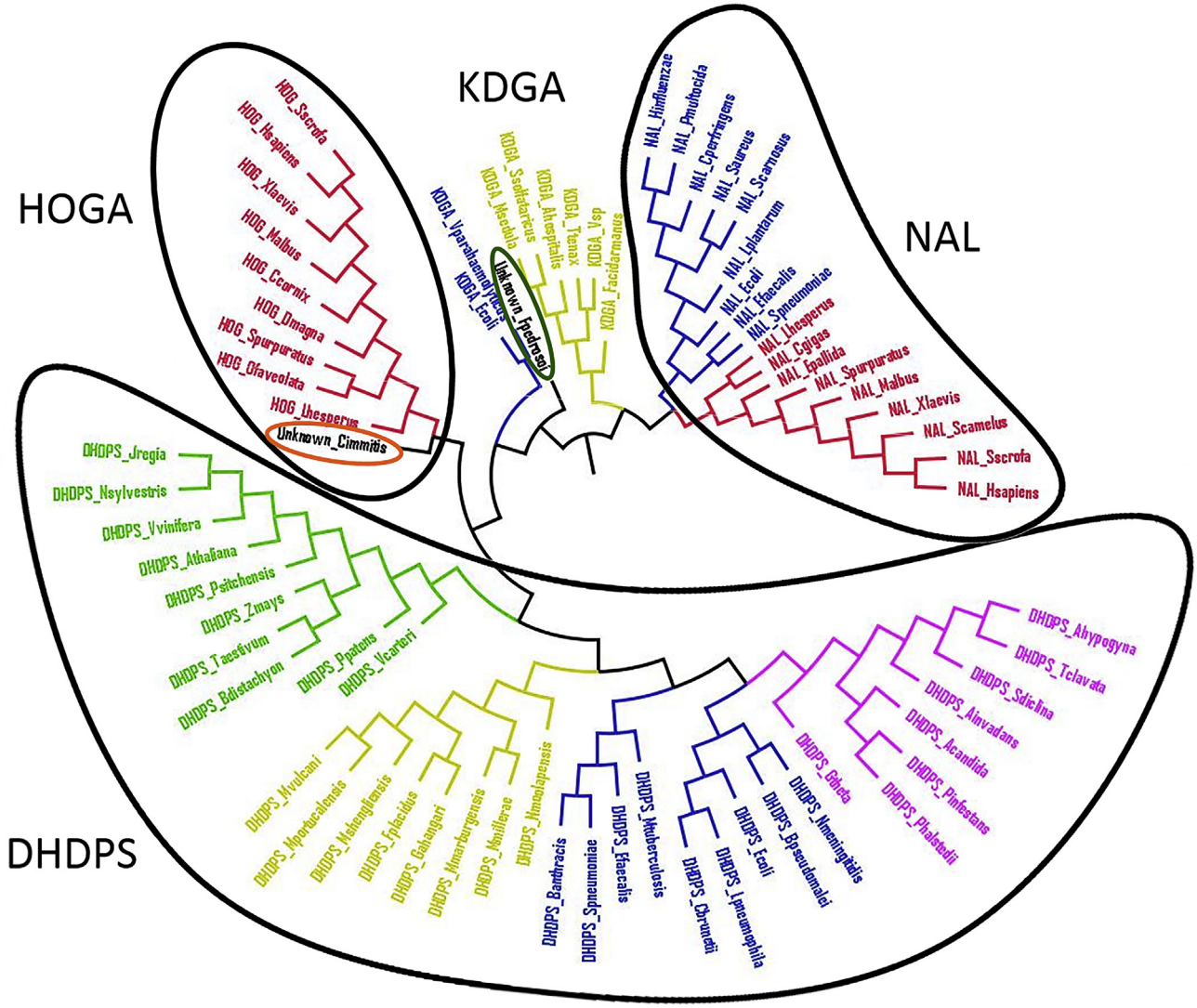

Fig. 7. Neighbor-joining phylogenetic tree of DHDPS, NAL, KDGA and HOGA sequences across kingdoms. The Animalia kingdom is represented in red, Archaea in yellow, Chromista in pink/purple, Eubacteria in blue and Planta in green. The fungus *C. immitis* sequence 3QFE is circled in orange and *F. pedrosoi* KIW77228 in dark green. The branches are not distant-defined.

earlier studies report that other enzymes functioning in the DAP pathway, namely DHDPR and diaminopimelate decarboxylase (DAPDC) (Fig. 1) are also lacking in Fungi [28]. We too could not find evidence in this study for the presence of *dapB* (i.e. DHDPR) or *lysA* (i.e. DAPDC) genes in contemporary fungal genome databases, which now encompass a total of 735 genomes from 444 fungal species (fungi.ensembl.org, www.broadinstitute.org/fungal-genome-initiative). This reinforces the notion that the DAP pathway is absent in Fungi, suggesting that this kingdom utilizes the AAA pathway instead to synthesize lysine.

3.9. Sequence analysis confirms fungi synthesize lysine using the AAA pathway

Although earlier studies suggest that some fungi use the DAP pathway to synthesize lysine [30–39], our results here demonstrate that this is not the case. A search of the NCBI and KEGG databases reveal that both *C. immitis* and *F. pedrosoi* possess all 7

Table 2
Accession numbers of all 7 α-aminoadipate (AAA) pathway enzymes from the fungi *C. immitis* and *F. pedrosoi*.

Enzyme Name	*C. immitis*	*F. pedrosoi*
Homocitrate synthase	KMU78670	KIW74236
Homoaconitase	KMU89268	KIW75522
Homoisocitrate dehydrogenase	KMU80207	KIW76394
α-Aminoadipate aminotransferase	KMU86282	XP_013287469
α-Aminoadipate reductase	KMU77278	KIW77788
Saccharopine dehydrogenase 1 (glutamate-forming)	EAS36201	KIW75793
Saccharopine dehydrogenase 2 (lysine-forming)	EAS34762	KIW83958

enzymes known to function in the AAA pathway (Table 2). Indeed, this is consistent with earlier reports suggesting that lysine biosynthesis in fungi occurs via the AAA pathway [2,27–29].

4. Conclusion

This study shows that 3QFE is not a DHDPS, but instead possesses dual HOGA/KDGA function with enzymatic activity comparable to those reported for single activity enzymes [73,82,101]. We propose a 7 residue signature (i.e. Thr44, Thr45, Tyr106, Tyr107, Tyr133, Arg138 & Lys161, *E. coli* numbering) that represents a DHDPS-specific motif; and show that even the absence of a single residue in this motif (i.e. Arg138) cannot support DHDPS function. Our results also indicate that no currently available fungal sequence possesses all 7 residues of this motif, supporting the notion that fungal genomes lack the *dapA* gene. Indeed, our study could not identify any fungal genes involved in DAP biosynthesis, confirming earlier reports that this pathway is absent in Fungi. However, we could identify all 7 genes functioning in the AAA pathway providing further evidence that Fungi only utilize this pathway to synthesize the essential amino acid, lysine. Importantly, this study highlights the need to employ validated functional sequence motifs to correctly assign class I aldolase sequences. This is critical to avoid gene misannotations as reported here and previously for *dapA* [63,73]. The need to implement robust methods for annotating genes by orthology rather than homology alone has been raised by prominent researchers in the field [112,113]. Furthermore, misannotations of fungal genes, including *dapA* pertinent to this study, is most likely the result of the recent reclassification of lower fungi as Chromista [114–116]. Future gene annotation efforts should therefore take into consideration: (i) orthology-assigned sequence motifs in addition to broad-base homology modelling; and less commonly, (ii) taxonomic reclassification of species, genus, family, order, class, phylum and even kingdom.

Acknowledgements

We thank Prof Juliet Gerard (University of Auckland, NZ) and A/Prof Renwick Dobson (University of Canterbury, NZ) for the *E. coli* DHDPS and *S. aureus* NAL clones, respectively. We would also like to thank A/Prof Ashley Franks (La Trobe University, Australia) for the AT997r$^-$ *E. coli* strain. We acknowledge the *La Trobe University-Comprehensive Proteomics Platform* for access to core mass spectrometry and CD spectroscopy equipment and expertise utilized in this study; and the Australian Research Council for providing discovery project funding (DP150103313). Lastly, we thank Dr Tatiana Soares da Costa and the rest of the Perugini lab for helpful discussion and comments during the preparation of this manuscript.

Appendix A. Supplementary data

Supplementary data related to this article can be found at https://doi.org/10.1016/j.biochi.2018.06.017.

Abbreviations

AAA	α-aminoadipate
AGRF	Australian Genome Research Facility
ASA	(S)-aspartate-4-semialdehyde
CD	circular dichroism
DAP	diaminopimelate
DAPDC	diaminopimelate decarboxylase
DHDPR	dihydrodipicolinate reductase
DHDPS	dihydrodipicolinate synthase
ESI	electrospray ionization
HOG	4-hydroxy-2-oxoglutarate
HOGA	4-hydroxy-2-oxoglutarate aldolase
HTPA	4-hydroxy-2,3,4,5-tetrahydrodipicolinic acid
IMAC	immobilized metal affinity chromatography
IPTG	isopropyl β-D-1-thiogalactopyranoside
KDG	2-keto-3-deoxygluconate
KDGA	2-keto-3-deoxygluconate aldolase
LB	Luria Broth
LDH	lactate dehydrogenase
ML	maximum likelihood
MRE	mean residue ellipticity
NAL	*N*-acetylneuraminate lyase
Neu5Ac	*N*-acetylneuraminic acid
NJ	neighbor joining
PDB	protein data bank
RF	radio frequency

References

[1] H.J. Vogel, Two modes of lysine synthesis among lower fungi: evolutionary significance, Biochim. Biophys. Acta 41 (1960) 172–173, https://doi.org/10.1016/0006-3002(60)90392-9.
[2] J.K. Bhattacharjee, α-aminoadipate pathway for the biosynthesis of lysine in lower eukaryotes, CRC Crit. Rev. Microbiol. 12 (1985) 131–151, https://doi.org/10.3109/10408418509104427.
[3] J.P. Townsend, D. Cavalieri, D.L. Hartl, Population genetic variation in genome-wide gene expression, Mol. Biol. Evol. 20 (2003) 955–963, https://doi.org/10.1093/molbev/msg106.
[4] C.A. Hutton, M.A. Perugini, J.A. Gerrard, Inhibition of lysine biosynthesis: an evolving antibiotic strategy, Mol. Biosyst. 3 (2007) 458, https://doi.org/10.1039/b705624a.
[5] Y. Yugari, C. Gilvarg, The condensation step in diaminopimelate synthesis, J. Biol. Chem. 240 (1965) 4710–4716.
[6] M. Ghislain, V. Frankard, M. Jacobs, Dihydrodipicolinate synthase of *Nicotiana sylvestris*, a chloroplast-localized enzyme of the lysine pathway, Planta 180 (1990) 480–486.
[7] C. Dereppe, G. Bold, O. Ghisalba, E. Ebert, H.-P. Schär, Purification and characterization of dihydrodipicolinate synthase from pea, Plant Physiol. 98 (1992) 813–821.
[8] B. Laber, F.X. Gomis-Ruth, M.J. Romao, R. Huber, Escherichia coli dihydrodipicolinate synthase. Identification of the active site and crystallization, Biochem. J. 288 (1992) 691–695.
[9] C. Mirwaldt, I. Korndorfer, R. Huber, The crystal structure of dihydrodipicolinate synthase from *Escherichia coli* at 2.5Å resolution, J. Mol. Biol. 246 (1995) 227–239.
[10] S. Blickling, H.-G. Beisel, D. Bozic, J. Knäblein, B. Laber, R. Huber, Structure of dihydrodipicolinate synthase of *Nicotiana sylvestris* reveals novel quaternary structure, J. Mol. Biol. 274 (1997) 608–621.
[11] S. Blickling, C. Renner, B. Laber, H.-D. Pohlenz, T.A. Holak, R. Huber, Reaction mechanism of *Escherichia coli* dihydrodipicolinate synthase investigated by X-ray crystallography and NMR spectroscopy, Biochemistry (Mosc.) 36 (1997) 24–33.
[12] R.C.J. Dobson, K. Valegård, J.A. Gerrard, The crystal structure of three site-directed mutants of *Escherichia coli* dihydrodipicolinate synthase: further evidence for a catalytic triad, J. Mol. Biol. 338 (2004) 329–339, https://doi.org/10.1016/j.jmb.2004.02.060.
[13] E. Blagova, V. Levdikov, N. Milioti, M.J. Fogg, A.K. Kalliomaa, J.A. Brannigan, et al., Crystal structure of dihydrodipicolinate synthase (BA3935) from *Bacillus anthracis* at 1.94 Å resolution, Proteins Struct. Funct. Bioinforma 62 (2006) 297–301, https://doi.org/10.1002/prot.20684.
[14] B.R. Burgess, R.C.J. Dobson, M.F. Bailey, S.C. Atkinson, M.D.W. Griffin, G.B. Jameson, et al., Structure and evolution of a novel dimeric enzyme from a clinically important bacterial pathogen, J. Biol. Chem. 283 (2008) 27598–27603, https://doi.org/10.1074/jbc.M804231200.
[15] M.D.W. Griffin, R.C.J. Dobson, F.G. Pearce, L. Antonio, A.E. Whitten, C.K. Liew, et al., Evolution of quaternary structure in a homotetrameric enzyme, J. Mol. Biol. 380 (2008) 691–703, https://doi.org/10.1016/j.jmb.2008.05.038.
[16] F. Kong, S. Jiang, X. Meng, C. Song, J. Shi, D. Jin, et al., Cloning and characterization of the DHDPS gene encoding the lysine biosynthetic enzyme dihydrodipocolinate synthase from *Zizania latifolia* (griseb), Plant Mol. Biol. Rep. 27 (2008) 199–208, https://doi.org/10.1007/s11105-008-0073-0.
[17] S. Wolterink-van Loo, M. Levisson, M.C. Cabrières, M.C.R. Franssen, Oost J van der. Characterization of a thermostable dihydrodipicolinate synthase from *Thermoanaerobacter tengcongensis*, Extremophiles 12 (2008) 461–469, https://doi.org/10.1007/s00792-008-0152-z.
[18] J.E. Voss, S.W. Scally, N.L. Taylor, S.C. Atkinson, M.D.W. Griffin, C.A. Hutton, et al., Substrate-mediated stabilization of a tetrameric drug target reveals achilles heel in anthrax, J. Biol. Chem. 285 (2010) 5188–5195, https://doi.org/10.1074/jbc.M109.038166.

[19] S.C. Atkinson, C. Dogovski, M.T. Downton, F.G. Pearce, C.F. Reboul, A.M. Buckle, et al., Crystal, solution and *in silico* structural studies of dihydrodipicolinate synthase from the common grapevine, PLoS One 7 (2012), e38318, https://doi.org/10.1371/journal.pone.0038318.

[20] C. Dogovski, S.C. Atkinson, S.R. Dommaraju, M. Downton, L. Hor, S. Moore, et al., Enzymology of bacterial lysine biosynthesis, Biochemist (2012) 225–262. InTech Open Access Publ., InTech.

[21] S.C. Atkinson, C. Dogovski, M.T. Downton, P.E. Czabotar, R.C.J. Dobson, J.A. Gerrard, et al., Structural, kinetic and computational investigation of *Vitis vinifera* DHDPS reveals new insight into the mechanism of lysine-mediated allosteric inhibition, Plant Mol. Biol. 81 (2013) 431–446, https://doi.org/10.1007/s11103-013-0014-7.

[22] E. Erzeel, P. Bochaute, T.T. Thu, G. Angenon, Medicago truncatula dihydrodipicolinate synthase (DHDPS) enzymes display novel regulatory properties, Plant Mol. Biol. 81 (2013) 401–415, https://doi.org/10.1007/s11103-013-0008-5.

[23] Y.V. Skovpen, D.R.J. Palmer, Dihydrodipicolinate synthase from *Campylobacter jejuni*: kinetic mechanism of cooperative allosteric inhibition and inhibitor-induced substrate cooperativity, Biochemistry (Mosc.) 52 (2013) 5454–5462, https://doi.org/10.1021/bi400693w.

[24] K. Kobayashi, S.D. Ehrlich, A. Albertini, G. Amati, K.K. Andersen, M. Arnaud, et al., Essential *Bacillus subtilis* genes, Proc. Natl. Acad. Sci. Unit. States Am. 100 (2003) 4678–4683.

[25] C. Dogovski, M.A. Gorman, N.E. Ketaren, J. Praszkier, L.M. Zammit, H.D. Mertens, et al., From knock-out phenotype to three-dimensional structure of a promising antibiotic target from *Streptococcus pneumoniae*, PLoS One 8 (2013), e83419, https://doi.org/10.1371/journal.pone.0083419.

[26] S. Jones-Held, L.P. Ambrozevicius, M. Campbell, B. Drumheller, E. Harrington, T. Leustek, Two *Arabidopsis thaliana* dihydrodipicolinate synthases, DHDPS1 and DHDPS2, are unequally redundant, Funct. Plant Biol. 39 (2012) 1058, https://doi.org/10.1071/FP12169.

[27] H. Xu, B. Andi, J. Qian, A.H. West, P.F. Cook, The α-aminoadipate pathway for lysine biosynthesis in fungi, Cell Biochem. Biophys. 46 (2006) 43–64.

[28] R. Guedes, F. Prosdocimi, G. Fernandes, L. Moura, H. Ribeiro, J. Ortega, Amino acids biosynthesis and nitrogen assimilation pathways: a great genomic deletion during eukaryotes evolution, BMC Genom. 12 (2011) 1–13, https://doi.org/10.1186/1471-2164-12-S4-S2.

[29] A.O. Hudson, M.A. Savka, F.G. Pearce, R.C.J. Dobson, Lysine biosynthesis in microorganisms, Handb. Microb. Metab. Amino Acids (2017) 49–69. CABI.

[30] D.R. Walters, A. McPherson, D.J. Robins, Inhibition of lysine biosynthesis in *Phytophthora infestans*, Mycol. Res. 101 (1997) 329–333, https://doi.org/10.1017/S0953756296002626.

[31] T.M. Zabriskie, M.D. Jackson, Lysine biosynthesis and metabolism in fungi, Nat. Prod. Rep. 17 (2000) 85–97.

[32] J. Acord, M. Masters, Expression from the *Escherichia coli dapA* promoter is regulated by intracellular levels of diaminopimelic acid, FEMS Microbiol. Lett. 235 (2004) 131–137, https://doi.org/10.1111/j.1574-6968.2004.tb09577.x.

[33] S.C. Atkinson, R.C.J. Dobson, J.M. Newman, M.A. Gorman, C. Dogovski, M.W. Parker, et al., Crystallization and preliminary X-ray analysis of dihydrodipicolinate synthase from *Clostridium botulinum* in the presence of its substrate pyruvate, Acta Crystallogr. F 65 (2009) 253–255, https://doi.org/10.1107/S1744309108039018.

[34] J.E. Voss, S.W. Scally, N.L. Taylor, C. Dogovski, M.R. Alderton, C.A. Hutton, et al., Expression, purification, crystallization and preliminary X-ray diffraction analysis of dihydrodipicolinate synthase from *Bacillus anthracis* in the presence of pyruvate, Acta Crystallogr. F 65 (2009) 188–191, https://doi.org/10.1107/S1744309109000670.

[35] N.E. Sibarani, M.A. Gorman, C. Dogovski, M.W. Parker, M.A. Perugini, Crystallization of dihydrodipicolinate synthase from a clinical isolate of *Streptococcus pneumoniae*, Acta Crystallograph Sect F Struct Biol Cryst Commun 66 (2010) 32–36, https://doi.org/10.1107/S174430910904771X.

[36] S.C. Atkinson, C. Dogovski, J. Newman, R.C.J. Dobson, M.A. Perugini, Cloning, expression, purification and crystallization of dihydrodipicolinate synthase from the grapevine *Vitis vinifera*, Acta Crystallograph Sect F Struct Biol Cryst Commun 67 (2011) 1537–1541, https://doi.org/10.1107/S1744309111038395.

[37] S.C. Atkinson, C. Dogovski, R.C.J. Dobson, M.A. Perugini, Cloning, expression, purification and crystallization of dihydrodipicolinate synthase from *Agrobacterium tumefaciens*, Acta Crystallograph Sect F Struct Biol Cryst Commun 68 (2012) 1040–1047, https://doi.org/10.1107/S1744309112033052.

[38] T. Siddiqui, J.J. Paxman, C. Dogovski, S. Panjikar, M.A. Perugini, Cloning to crystallization of dihydrodipicolinate synthase from the intracellular pathogen *Legionella pneumophila*, Acta Crystallograph Sect F Struct Biol Cryst Commun 69 (2013) 1177–1181, https://doi.org/10.1107/S1744309113024639.

[39] F.G. Pearce, A.O. Hudson, K. Loomes, R.C.J. Dobson, Dihydrodipicolinate synthase: structure, dynamics, function, and evolution, in: J.R. Harris, J. Marles-Wright (Eds.), Macromol. Protein Complexes, vol. 83, Springer International Publishing, Cham, 2017, pp. 271–289, https://doi.org/10.1007/978-3-319-46503-6_10.

[40] J.B. Christensen, T.P. Soares da Costa, P. Faou, F.G. Pearce, S. Panjikar, M.A. Perugini, Structure and function of cyanobacterial DHDPS and DHDPR, Sci. Rep. 6 (2016), https://doi.org/10.1038/srep37111.

[41] K.F. Naqvi, B.L. Staker, R.C.J. Dobson, D. Serbzhinskiy, B. Sankaran, P.J. Myler, et al., Cloning, expression, purification, crystallization and X-ray diffraction analysis of dihydrodipicolinate synthase from the human pathogenic bacterium *Bartonella henselae* strain Houston-1 at 2.1 Å resolution, Acta Crystallogr Sect F Struct Biol Commun 72 (2016) 2–9, https://doi.org/10.1107/S2053230X15023213.

[42] C.J.T. Conly, Y.V. Skovpen, S. Li, D.R.J. Palmer, D.A.R. Sanders, Tyrosine 110 plays a critical role in regulating the allosteric inhibition of *Campylobacter jejuni* dihydrodipicolinate synthase by lysine, Biochemistry (Mosc.) 53 (2014) 7396–7406, https://doi.org/10.1021/bi5012157.

[43] Y.V. Skovpen, C.J.T. Conly, D.A.R. Sanders, D.R.J. Palmer, Biomimetic design results in a potent allosteric inhibitor of dihydrodipicolinate synthase from *Campylobacter jejuni*, J. Am. Chem. Soc. 138 (2016) 2014–2020, https://doi.org/10.1021/jacs.5b12695.

[44] E.A. Rice, G.A. Bannon, K.C. Glenn, S.S. Jeong, E.J. Sturman, T.J. Rydel, Characterization and crystal structure of lysine insensitive *Corynebacterium glutamicum* dihydrodipicolinate synthase (cDHDPS) protein, Arch. Biochem. Biophys. 480 (2008) 111–121, https://doi.org/10.1016/j.abb.2008.09.018.

[45] R.C.J. Dobson, M.D.W. Griffin, G.B. Jameson, J.A. Gerrard, The crystal structures of native and (*S*)-lysine-bound dihydrodipicolinate synthase from *Escherichia coli* with improved resolution show new features of biological significance, Acta Crystallogr D Biol Crystallogr 61 (2005) 1116–1124, https://doi.org/10.1107/S0907444905016318.

[46] R.C.J. Dobson, S.R.A. Devenish, L.A. Turner, V.R. Clifford, F.G. Pearce, G.B. Jameson, et al., Role of arginine 138 in the catalysis and regulation of *Escherichia coli* dihydrodipicolinate synthase, Biochemistry (Mosc.) 44 (2005) 13007–13013, https://doi.org/10.1021/bi051281w.

[47] S.R.A. Devenish, J.A. Gerrard, G.B. Jameson, R.C.J. Dobson, The high-resolution structure of dihydrodipicolinate synthase from *Escherichia coli* bound to its first substrate, pyruvate, Acta Crystallogr. F 64 (2008) 1092–1095, https://doi.org/10.1107/S1744309108033654.

[48] R.C.J. Dobson, M.D.W. Griffin, S.R.A. Devenish, F.G. Pearce, C.A. Hutton, J.A. Gerrard, et al., Conserved main-chain peptide distortions: a proposed role for Ile203 in catalysis by dihydrodipicolinate synthase, Protein Sci. 17 (2008) 2080–2090, https://doi.org/10.1110/ps.037440.108.

[49] F.G. Pearce, R.C.J. Dobson, A. Weber, L.A. Lane, M.G. McCammon, M.A. Squire, et al., Mutating the tight-dimer interface of dihydrodipicolinate synthase disrupts the enzyme quaternary structure: toward a monomeric enzyme, Biochemistry (Mosc.) 47 (2008) 12108–12117, https://doi.org/10.1021/bi801094t.

[50] R.C.J. Dobson, M.A. Perugini, G.B. Jameson, J.A. Gerrard, Specificity versus catalytic potency: the role of threonine 44 in *Escherichia coli* dihydrodipicolinate synthase mediated catalysis, Biochimie 91 (2009) 1036–1044, https://doi.org/10.1016/j.biochi.2009.05.013.

[51] T.P. Soares da Costa, A.C. Muscroft-Taylor, R.C.J. Dobson, S.R.A. Devenish, G.B. Jameson, J.A. Gerrard, How essential is the 'essential' active-site lysine in dihydrodipicolinate synthase? Biochimie 92 (2010) 837–845, https://doi.org/10.1016/j.biochi.2010.03.004.

[52] G. Kefala, G.L. Evans, M.D.W. Griffin, S.R.A. Devenish, F.G. Pearce, M.A. Perugini, et al., Crystal structure and kinetic study of dihydrodipicolinate synthase from *Mycobacterium tuberculosis*, Biochem. J. 411 (2008) 351, https://doi.org/10.1042/BJ20071360.

[53] P. Shrivastava, V. Navratna, Y. Silla, R.P. Dewangan, A. Pramanik, S. Chaudhary, et al., Inhibition of *Mycobacterium tuberculosis* dihydrodipicolinate synthase by α-ketopimelic acid and its other structural analogues, Sci. Rep. 6 (2016) 30827, https://doi.org/10.1038/srep30827.

[54] S.R.A. Devenish, F.H.A. Huisman, E.J. Parker, A.T. Hadfield, J.A. Gerrard, Cloning and characterisation of dihydrodipicolinate synthase from the pathogen *Neisseria meningitidis*, Biochim Biophys Acta BBA - Proteins Proteomics 1794 (2009) 1168–1174, https://doi.org/10.1016/j.bbapap.2009.02.003.

[55] N. Kaur, A. Gautam, S. Kumar, A. Singh, N. Singh, S. Sharma, et al., Biochemical studies and crystal structure determination of dihydrodipicolinate synthase from *Pseudomonas aeruginosa*, Int. J. Biol. Macromol. 48 (2011) 779–787, https://doi.org/10.1016/j.ijbiomac.2011.03.002.

[56] R. Schnell, W. Oehlmann, T. Sandalova, Y. Braun, C. Huck, M. Maringer, et al., Tetrahydrodipicolinate N-Succinyltransferase and dihydrodipicolinate synthase from *Pseudomonas aeruginosa*: structure analysis and gene deletion, PLoS One 7 (2012), e31133, https://doi.org/10.1371/journal.pone.0031133.

[57] B.R. Burgess, R.C.J. Dobson, C. Dogovski, G.B. Jameson, M.W. Parker, M.A. Perugini, Purification, crystallization and preliminary X-ray diffraction studies to near-atomic resolution of dihydrodipicolinate synthase from methicillin-resistant *Staphylococcus aureus*, Acta Crystallograph Sect F Struct Biol Cryst Commun 64 (2008) 659–661, https://doi.org/10.1107/S1744309108016746.

[58] T.S. Girish, E. Sharma, B. Gopal, Structural and functional characterization of *Staphylococcus aureus* dihydrodipicolinate synthase, FEBS Lett. 582 (2008) 2923–2930, https://doi.org/10.1016/j.febslet.2008.07.035.

[59] F.G. Pearce, R.C.J. Dobson, G.B. Jameson, M.A. Perugini, J.A. Gerrard, Characterization of monomeric dihydrodipicolinate synthase variant reveals the importance of substrate binding in optimizing oligomerization, Biochim Biophys Acta BBA - Proteins Proteomics 1814 (2011) 1900–1909, https://doi.org/10.1016/j.bbapap.2011.07.016.

[60] M.D.W. Griffin, J.M. Billakanti, A. Wason, S. Keller, H.D.T. Mertens, S.C. Atkinson, et al., Characterisation of the first enzymes committed to lysine biosynthesis in *Arabidopsis thaliana*, PLoS One 7 (2012), e40318, https://

doi.org/10.1371/journal.pone.0040318.
[61] B. Padmanabhan, R.W. Strange, S.V. Antonyuk, M.J. Ellis, S.S. Hasnain, H. Iino, et al., Structure of dihydrodipicolinate synthase from *Methanocaldococcus jannaschii*, Acta Crystallograph Sect F Struct Biol Cryst Commun 65 (2009) 1222–1226, https://doi.org/10.1107/S174430910904651X.
[62] T.P. Soares da Costa, J.B. Christensen, S. Desbois, S.E. Gordon, R. Gupta, C.J. Hogan, et al., Quaternary structure analyses of an essential oligomeric enzyme, Methods Enzymol. 562 (2015) 205–223. Elsevier.
[63] S.C. Atkinson, L. Hor, C. Dogovski, R.C.J. Dobson, M.A. Perugini, Identification of the *bona fide* DHDPS from a common plant pathogen, Proteins Struct. Funct. Bioinforma 82 (2014) 1869–1883, https://doi.org/10.1002/prot.24539.
[64] S.E. Gordon, D.K. Weber, M.T. Downton, J. Wagner, M.A. Perugini, Dynamic modelling reveals 'hotspots' on the pathway to enzyme-substrate complex formation, PLoS Comput. Biol. 12 (2016), e1004811, https://doi.org/10.1371/journal.pcbi.1004811.
[65] M.A. Perugini, M.D.W. Griffin, B.J. Smith, L.E. Webb, A.J. Davis, E. Handman, et al., Insight into the self-association of key enzymes from pathogenic species, Eur. Biophys. J. 34 (2005) 469–476, https://doi.org/10.1007/s00249-005-0491-y.
[66] T.N. Kirkland, J. Fierer, Coccidioidomycosis: a reemerging infectious disease, Emerg. Infect. Dis. 2 (1996) 192–199.
[67] V. Koufopanou, A. Burt, T. Szaro, J.W. Taylor, Gene genealogies, cryptic species, and molecular evolution in the human pathogen Coccidioides immitis and relatives (ascomycota, onygenales), Mol. Biol. Evol. 18 (2001) 1246–1258, https://doi.org/10.1093/oxfordjournals.molbev.a003910.
[68] J. Brown, K. Benedict, B.J. Park, G.R. Thompson, Coccidioidomycosis: epidemiology, Clin. Epidemiol. 5 (2013) 185–197, https://doi.org/10.2147/CLEP.S34434.
[69] T. Kaneko, T. Hashimoto, R. Kumpaisal, Y. Yamada, Molecular cloning of wheat dihydrodipicolinate synthase, J. Biol. Chem. 265 (1990) 17451–17455.
[70] M. Vauterin, V. Frankard, M. Jacobs, The *Arabidopsis thaliana dhdps* gene encoding dihydrodipicolinate synthase, key enzyme of lysine biosynthesis, is expressed in a cell-specific manner, Plant Mol. Biol. 39 (1999) 695–708.
[71] A. Craciun, M. Jacobs, M. Vauterin, Arabidopsis loss-of-function mutant in the lysine pathway points out complex regulation mechanisms, FEBS Lett. 487 (2000) 234–238, https://doi.org/10.1016/S0014-5793(00)02303-6.
[72] C. Sarrobert, M.-C. Thibaud, P. Contard-David, S. Gineste, N. Bechtold, C. Robaglia, et al., Identification of an *Arabidopsis thaliana* mutant accumulating threonine resulting from mutation in a new dihydrodipicolinate synthase gene, Plant J. 24 (2000) 357–368, https://doi.org/10.1046/j.1365-313x.2000.00884.x.
[73] T.P. Soares da Costa, M. Patel, S. Desbois, R. Gupta, P. Faou, M.A. Perugini, Identification of a dimeric KDG aldolase from *Agrobacterium tumefaciens*, Proteins Struct. Funct. Bioinforma 85 (2017) 2058–2065, https://doi.org/10.1002/prot.25359.
[74] S. Zhang, G. Zubay, E. Goldman, Low-usage codons in *Escherichia coli*, yeast, fruit fly and primates, Gene 105 (1991) 61–72.
[75] F. Sanger, S. Nicklen, A.R. Coulson, DNA sequencing with chain-terminating inhibitors, Proc. Natl. Acad. Sci. Unit. States Am. 74 (1977) 5463–5467.
[76] J. Sambrook, D.W. Russell, Molecular Cloning, a Laboratory Manual, third ed., vol. 3, Cold Spring Harbor Laboratory Press, 2001.
[77] N. Sreerama, S.Y. Venyaminov, R.W. Woody, Estimation of protein secondary structure from circular dichroism spectra: inclusion of denatured proteins with native proteins in the analysis, Anal. Biochem. 287 (2000) 243–251, https://doi.org/10.1006/abio.2000.4879.
[78] N. Sreerama, R.W. Woody, Estimation of protein secondary structure from circular dichroism spectra: comparison of CONTIN, SELCON, and CDSSTR methods with an expanded reference set, Anal. Biochem. 287 (2000) 252–260, https://doi.org/10.1006/abio.2000.4880.
[79] C.V. Coulter, J.A. Gerrard, J.A.E. Kraunsoe, A.J. Pratt, Escherichia coli dihydrodipicolinate synthase and dihydrodipicolinate reductase: kinetic and inhibition studies of two putative herbicide targets, Pestic. Sci. 55 (1999) 887–895.
[80] T.P. Soares da Costa, S. Desbois, C. Dogovski, M.A. Gorman, N.E. Ketaren, J.J. Paxman, et al., Structural determinants defining the allosteric inhibition of an essential antibiotic target, Structure 24 (2016) 1282–1291, https://doi.org/10.1016/j.str.2016.05.019.
[81] R.A. North, A.J.A. Watson, F.G. Pearce, A.C. Muscroft-Taylor, R. Friemann, A.J. Fairbanks, et al., Structure and inhibition of N-acetylneuraminate lyase from methicillin-resistant *Staphylococcus aureus*, FEBS Lett. 590 (2016) 4414–4428, https://doi.org/10.1002/1873-3468.12462.
[82] T.J. Riedel, L.C. Johnson, J. Knight, R.R. Hantgan, R.P. Holmes, W.T. Lowther, Structural and biochemical studies of human 4-hydroxy-2-oxoglutarate aldolase: implications for hydroxyproline metabolism in primary hyperoxaluria, PLoS One 6 (2011), e26021, https://doi.org/10.1371/journal.pone.0026021.
[83] T.J. Riedel, J. Knight, M.S. Murray, D.S. Milliner, R.P. Holmes, W.T. Lowther, 4-Hydroxy-2-oxoglutarate aldolase inactivity in primary hyperoxaluria type 3 and glyoxylate reductase inhibition, Biochim Biophys Acta BBA - Mol Basis Dis 1822 (2012) 1544–1552, https://doi.org/10.1016/j.bbadis.2012.06.014.
[84] A.I. Bukhari, A.L. Taylor, Genetic analysis of diaminopimelic acid- and lysine-requiring mutants of *Escherichia coli*, J. Bacteriol. 105 (1971) 844–854.
[85] P. Yeh, A.M. Sicard, A.J. Sinskey, General organization of the genes specifically involved in the diaminopimelate-lysine biosynthetic pathway of *Corynebacterium glutamicum*, Mol. Gen. Genet. MGG 212 (1988) 105–111, https://doi.org/10.1007/BF00322451.
[86] F.M. García-Rodríguez, S. Zekri, N. Toro, Characterization of the *Sinorhizobium meliloti* genes encoding a functional dihydrodipicolinate synthase (*dapA*) and dihydrodipicolinate reductase (*dapB*), Arch. Microbiol. 173 (2000) 438–444, https://doi.org/10.1007/s002030000169.
[87] J.D. Thompson, D.G. Higgins, T.J. Gibson, CLUSTAL: W improving the sensitivity of progressive multiple sequence alignment through sequence weighting, position-specific gap penalties and weight matrix choice, Nucleic Acids Res. 22 (1994) 4673–4680, https://doi.org/10.1093/nar/22.22.4673.
[88] N. Saitou, M. Nei, The neighbor-joining method: a new method for reconstructing phylogenetic trees, Mol. Biol. Evol. 4 (1987) 406–425, https://doi.org/10.1093/oxfordjournals.molbev.a040454.
[89] J. Felsenstein, Evolutionary trees from gene frequencies and quantitative characters: finding maximum likelihood estimates, Evolution 35 (1981) 1229–1242, https://doi.org/10.1111/j.1558-5646.1981.tb04991.x.
[90] J. Felsenstein, Evolutionary trees from DNA sequences: a maximum likelihood approach, J. Mol. Evol. 17 (1981) 368–376, https://doi.org/10.1007/BF01734359.
[91] K. Tamura, G. Stecher, D. Peterson, A. Filipski, S. Kumar, MEGA6: molecular evolutionary genetics analysis version 6.0, Mol. Biol. Evol. 30 (2013) 2725–2729, https://doi.org/10.1093/molbev/mst197.
[92] M. Nei, Molecular Evolutionary Genetics, Columbia University Press, New York, 1987.
[93] D.T. Jones, W.R. Taylor, J.M. Thornton, The rapid generation of mutation data matrices from protein sequences, Bioinformatics 8 (1992) 275–282, https://doi.org/10.1093/bioinformatics/8.3.275.
[94] B. DasGupta, X. He, T. Jiang, M. Li, J. Tromp, L. Zhang, On computing the nearest neighbor interchange distance, Discrete Math. Probl. Med. Appl. 55 (2000) 125–145. U.S.A.: American Mathematical Society.
[95] J. Felsenstein, Inferring Phylogenies, vol. 2, Sinauer associates Sunderland, MA, Washington, 2004.
[96] B.J. Smith, M.C. Lawrence, J.A.R.G. Barbosa, Substrate-assisted catalysis in sialic acid aldolase, J. Org. Chem. 64 (1999) 945–949, https://doi.org/10.1021/jo981960v.
[97] J.A.R.G. Barbosa, B.J. Smith, R. DeGori, H.C. Ooi, S.M. Marcuccio, E.M. Campi, et al., Active site modulation in the N-acetylneuraminate lyase sub-family as revealed by the structure of the inhibitor-complexed Haemophilus influenzae enzyme, J. Mol. Biol. 303 (2000) 405–421, https://doi.org/10.1006/jmbi.2000.4138.
[98] A.C. Joerger, S. Mayer, A.R. Fersht, Mimicking natural evolution in vitro: an N-acetylneuraminate lyase mutant with an increased dihydrodipicolinate synthase activity, Proc. Natl. Acad. Sci. Unit. States Am. 100 (2003) 5694–5699.
[99] G. Sánchez-Carrón, M.I. García-García, A.B. López-Rodríguez, S. Jiménez-García, A. Sola-Carvajal, F. García-Carmona, et al., Molecular characterization of a novel N-Acetylneuraminate lyase from lactobacillus plantarum WCFS1, Appl. Environ. Microbiol. 77 (2011) 2471–2478, https://doi.org/10.1128/AEM.02927-10.
[100] A.D. Daniels, I. Campeotto, M.W. van der Kamp, A.H. Bolt, C.H. Trinh, S.E.V. Phillips, et al., Reaction mechanism of N-Acetylneuraminic acid lyase revealed by a combination of crystallography, QM/mm simulation, and mutagenesis, ACS Chem. Biol. 9 (2014) 1025–1032, https://doi.org/10.1021/cb500067z.
[101] E.E. Dekker, R.P. Kitson, 2-Keto-4-hydroxyglutarate aldolase: purification and characterization of the homogeneous enzyme from bovine kidney, J. Biol. Chem. 267 (1992) 10507–10514.
[102] J. Jia, W. Huang, U.S. rken, H. Sahm, G.A. Sprenger, Y. Lindqvist, et al., Crystal structure of transaldolase B from Escherichia coli suggests a circular permutation of the α/β barrel within the class I aldolase family, Structure 4 (1996) 715–724, https://doi.org/10.1016/S0969-2126(96)00077-9.
[103] A.K. Samland, G.A. Sprenger, Microbial aldolases as C–C bonding enzymes—unknown treasures and new developments, Appl. Microbiol. Biotechnol. 71 (2006) 253, https://doi.org/10.1007/s00253-006-0422-6.
[104] P. Clapés, W.-D. Fessner, G.A. Sprenger, A.K. Samland, Recent progress in stereoselective synthesis with aldolases, Curr. Opin. Chem. Biol. 14 (2010) 154–167, https://doi.org/10.1016/j.cbpa.2009.11.029.
[105] S. Wolterink-van Loo, A. van Eerde, M.A.J. Siemerink, J. Akerboom, B.W. Dijkstra, J. van der Oost, Biochemical and structural exploration of the catalytic capacity of Sulfolobus KDG aldolases, Biochem. J. 403 (2007) 421–430, https://doi.org/10.1042/BJ20061419.
[106] T.J.G. Ettema, H. Ahmed, A.C.M. Geerling, Oost J. van der, B. Siebers, The non-phosphorylating glyceraldehyde-3-phosphate dehydrogenase (GAPN) of Sulfolobus solfataricus: a key-enzyme of the semi-phosphorylative branch of the Entner–Doudoroff pathway, Extremophiles 12 (2008) 75–88, https://doi.org/10.1007/s00792-007-0082-1.
[107] A.K. Samland, M. Wang, G.A. Sprenger, MJ0400 from Methanocaldococcus jannaschii exhibits fructose-1,6-bisphosphate aldolase activity, FEMS Microbiol. Lett. 281 (2008) 36–41, https://doi.org/10.1111/j.1574-6968.2008.01079.x.
[108] A. Flechner, W. Gross, W.F. Martin, C. Schnarrenberger, Chloroplast class I and class II aldolases are bifunctional for fructose-1,6-biphosphate and sedoheptulose-1,7-biphosphate cleavage in the Calvin cycle, FEBS Lett. 447 (1999) 200–202, https://doi.org/10.1016/S0014-5793(99)00285-9.
[109] Z. Zhang, W. Miller, A.A. Schäffer, T.L. Madden, D.J. Lipman, E.V. Koonin, et al.,

Protein sequence similarity searches using patterns as seeds, Nucleic Acids Res. 26 (1998) 3986–3990, https://doi.org/10.1093/nar/26.17.3986.
[110] S.F. Altschul, T.L. Madden, A.A. Schäffer, J. Zhang, Z. Zhang, W. Miller, et al., Gapped BLAST and PSI-BLAST: a new generation of protein database search programs, Nucleic Acids Res. 25 (1997) 3389–3402, https://doi.org/10.1093/nar/25.17.3389.
[111] M.J. Najafzadeh, J. Sun, V.A. Vicente, C.H.W. Klaassen, A. Bonifaz, A.H.G.G. van den Ende, et al., Molecular epidemiology of Fonsecaea species, Emerg. Infect. Dis. 17 (2011) 464–469, https://doi.org/10.3201/1703.100555.
[112] K. Gori, T. Suchan, N. Alvarez, N. Goldman, C. Dessimoz, Clustering genes of common evolutionary history, Mol. Biol. Evol. 33 (2016) 1590–1605, https://doi.org/10.1093/molbev/msw038.
[113] J. Huerta-Cepas, K. Forslund, L.P. Coelho, D. Szklarczyk, L.J. Jensen, C. von Mering, et al., Fast genome-wide functional annotation through orthology assignment by eggNOG-mapper, Mol. Biol. Evol. 34 (2017) 2115–2122, https://doi.org/10.1093/molbev/msx148.
[114] T. Cavalier-Smith, D.J. Chadwick, J. Whelan, Origins of Secondary Metabolism. Second. Metab. Their Funct. Evol, John Wiley & Sons, 1992, pp. 64–87.
[115] D.L. Hawksworth, P.M. Kirk, B.C. Sutton, D.N. Pegler, Ainsworth & Bisby's Dictionary of the Fungi, eighth ed., CABI, 1996.
[116] M.A. Ruggiero, D.P. Gordon, T.M. Orrell, N. Bailly, T. Bourgoin, R.C. Brusca, et al., A higher level classification of all living organisms, PLoS One 10 (2015), e0119248.